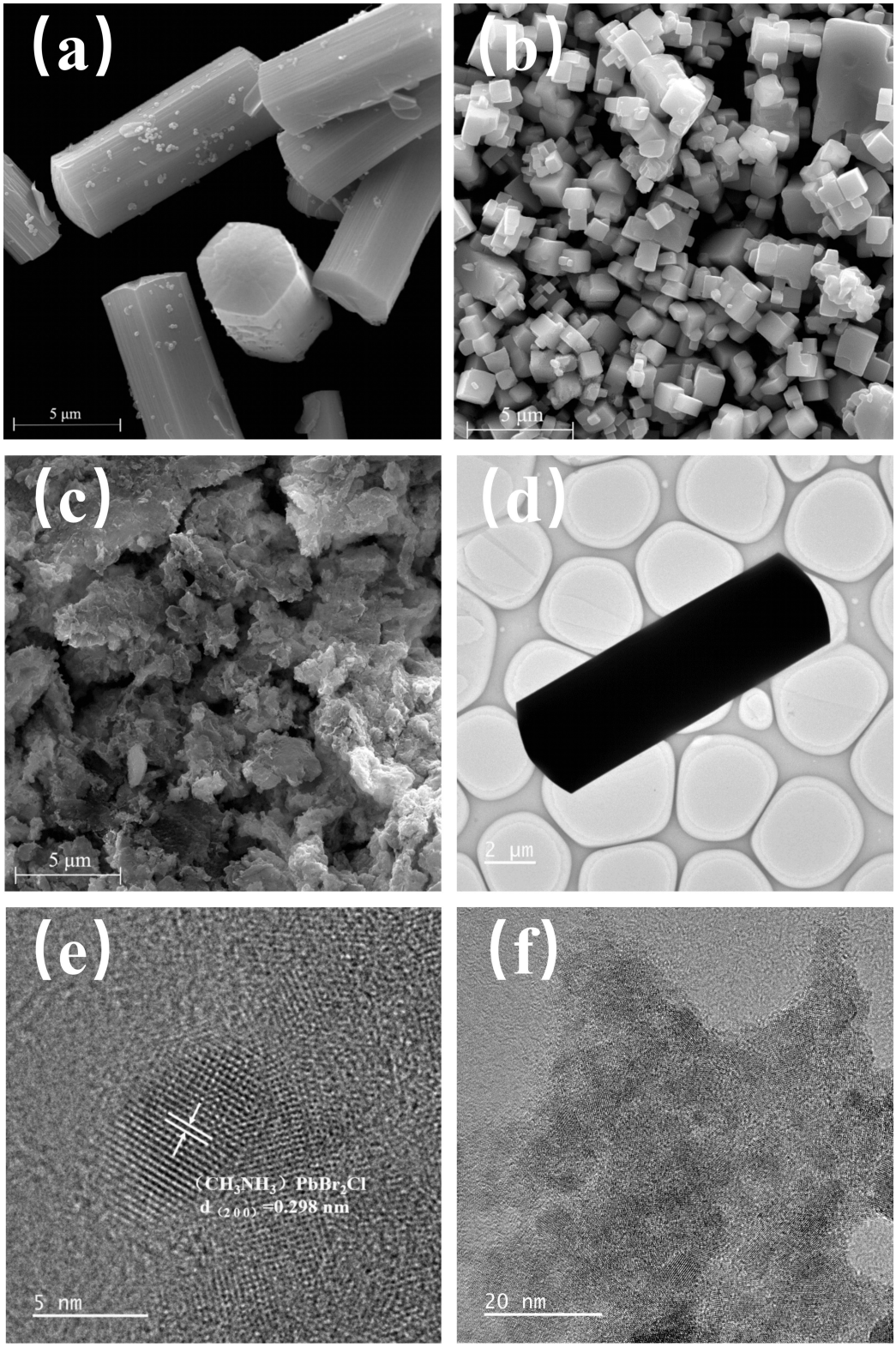

Fig.S1 SEM image of (a) CAU-17, (b) MAPbBr2Cl (c) CM-80 and TEM image of (d) CAU-17, (e-f) CM-80 sample

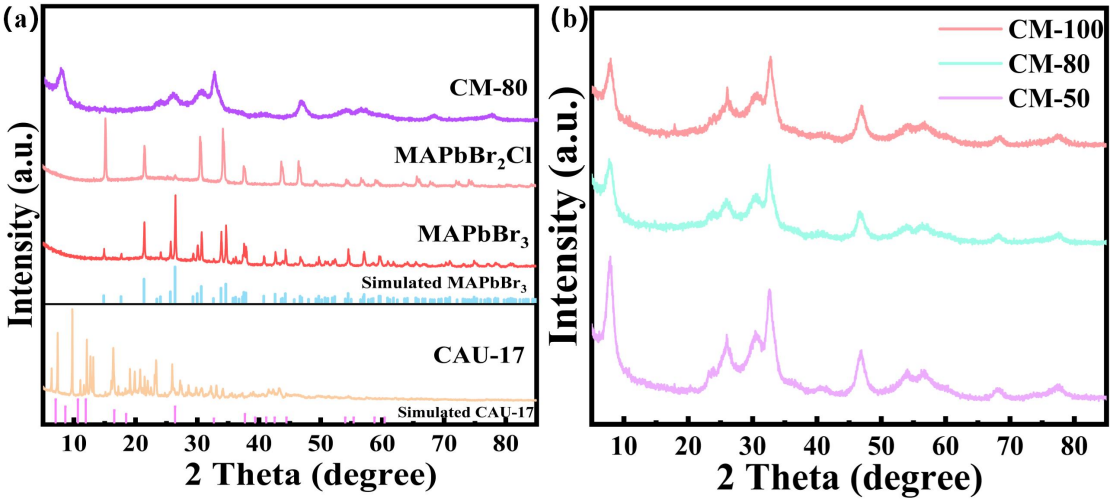

Fig.2 XRD spectra of CAU-17, MAPbBr2Cl and CM-X materials

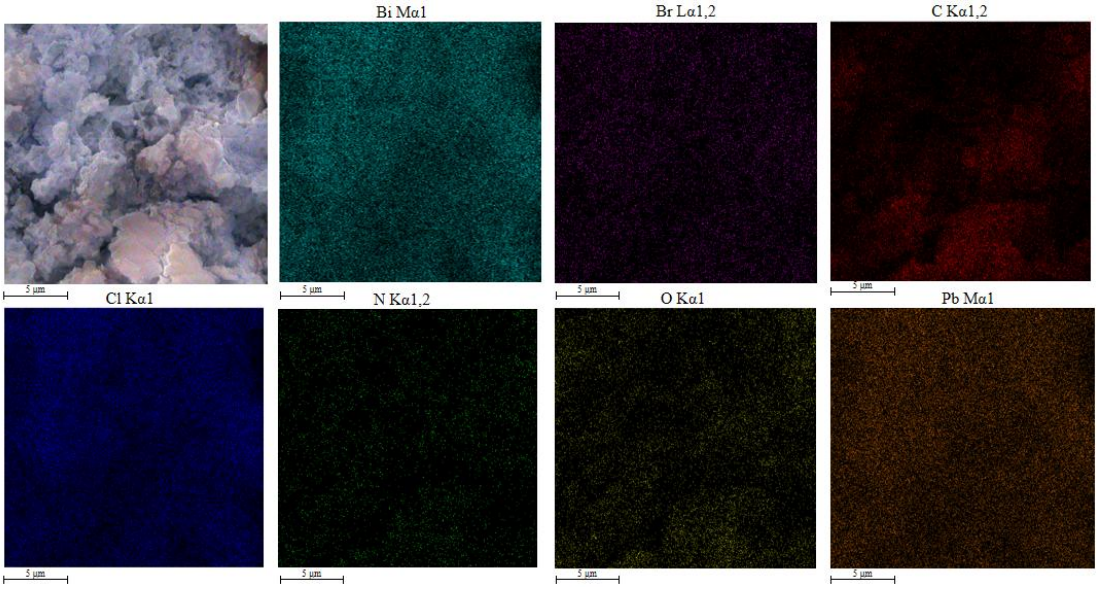

Fig.S3 SEM mapping of element distribution of CM-80 material

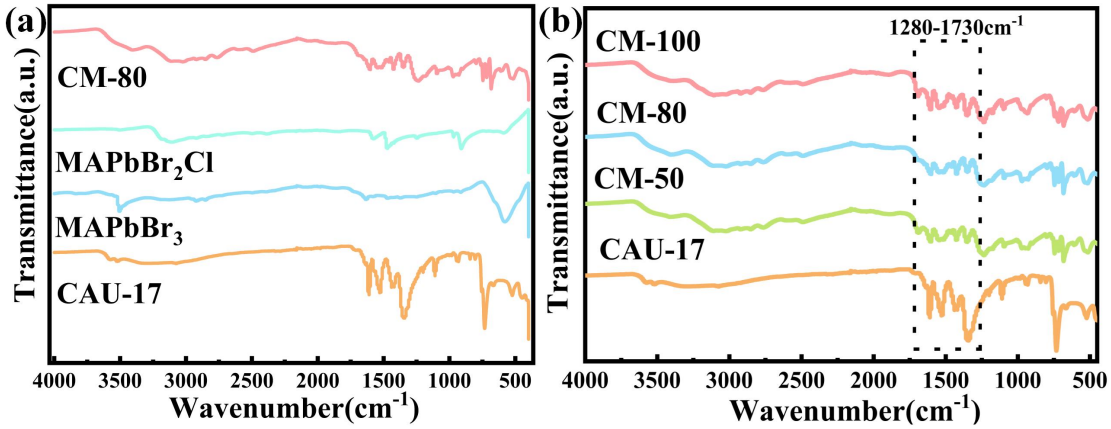

Fig.S4 FTIR spectra of CAU-17, $MAPbBr_2Cl$ and CM-X materials

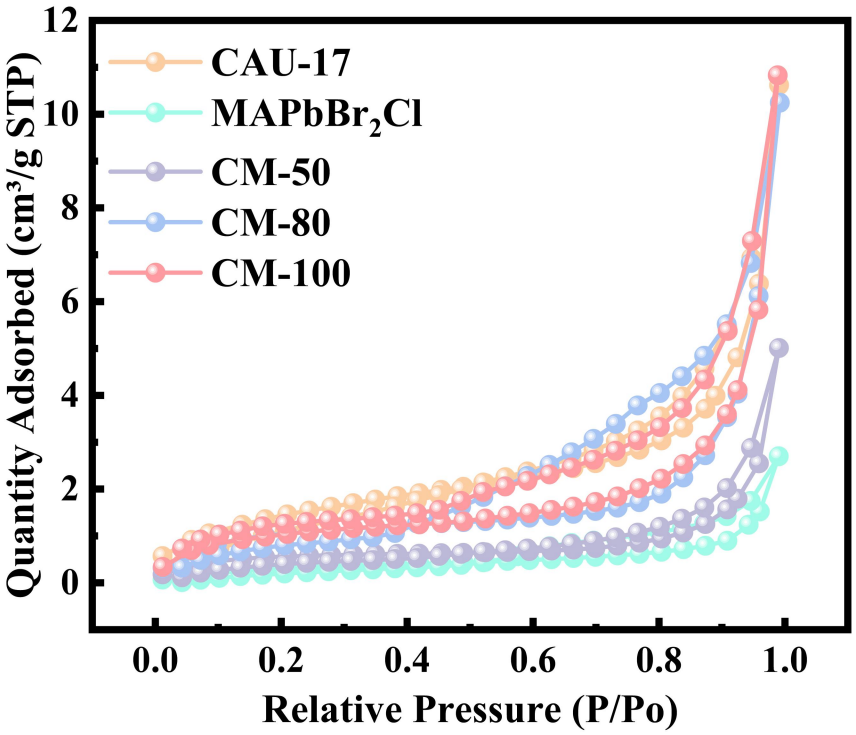

Fig.S5 N_2 adsorption-desorption isotherms of CAU-17, $MAPbBr_2Cl$ and CM-X materials

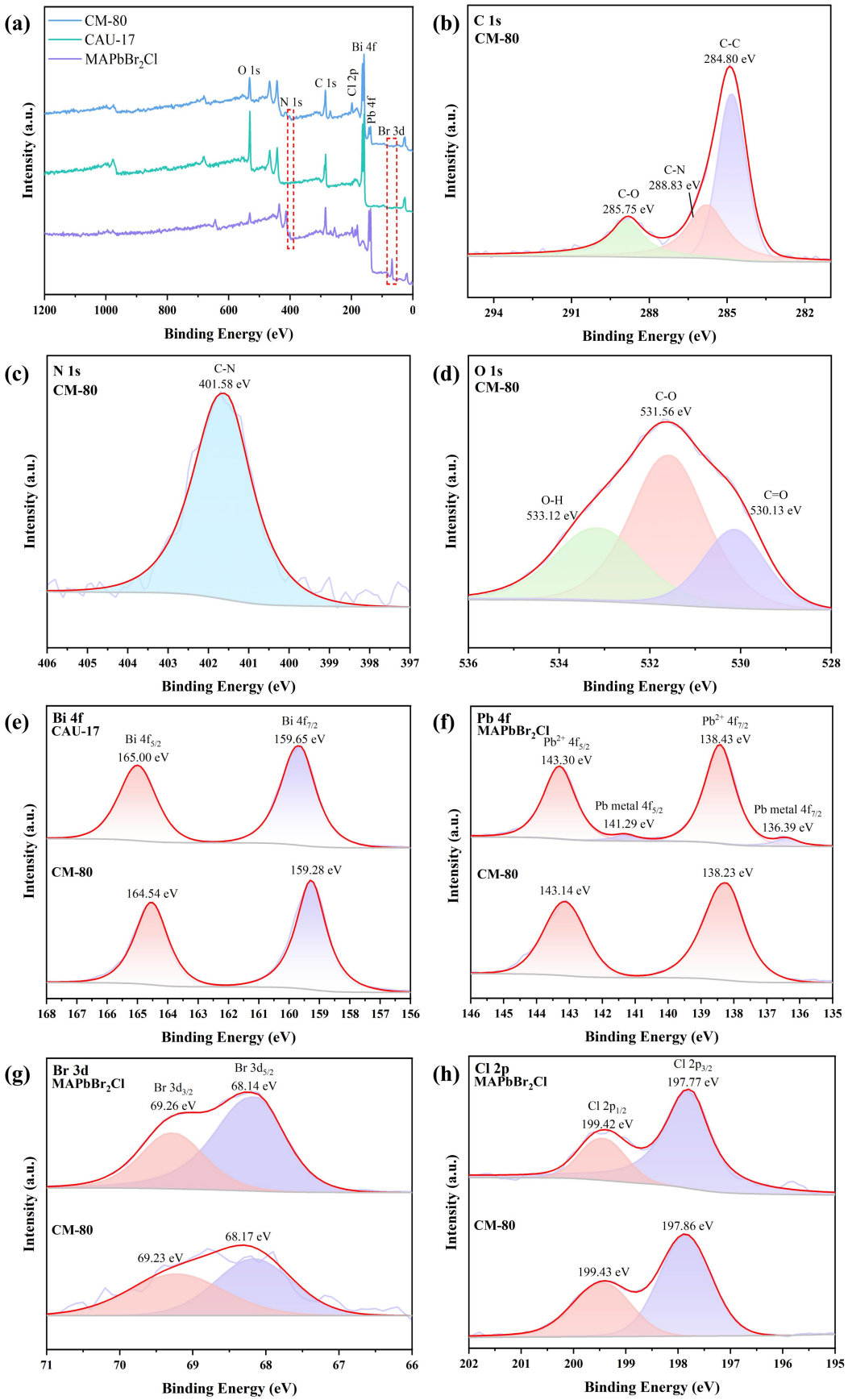

Fig.S6 XPS spectra of CAU-17, $MAPbBr_2Cl$ and CM-80 materials: (a) total spectrum, (b) C1s, (c) N 1s, (d) O 1s, (e) Bi 4f, (f) Pb 4f, (g) Br 3d, (h)Cl 2p

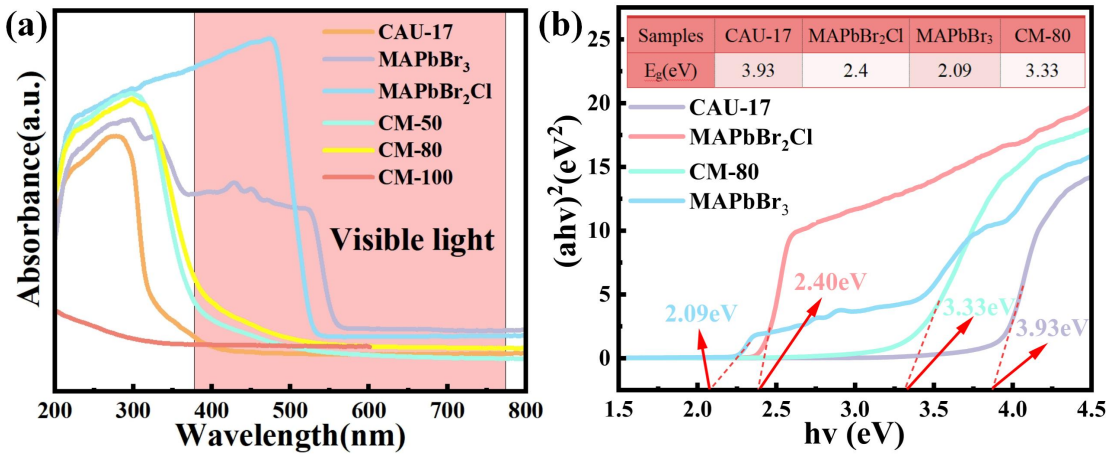

Fig.S7 (a) UV-VIS diffuse reflection spectrum of the prepared material; (b) Comparison of bandgap widths of different materials

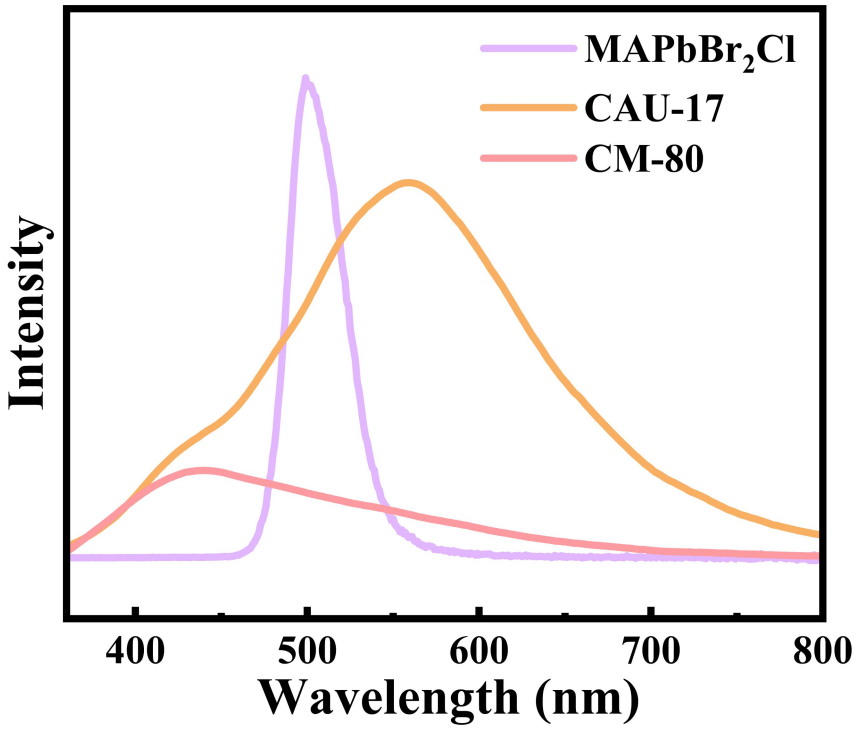

Fig.S8 PL spectra of CAU-17, MAPbBr2Cl and CM-80 materials

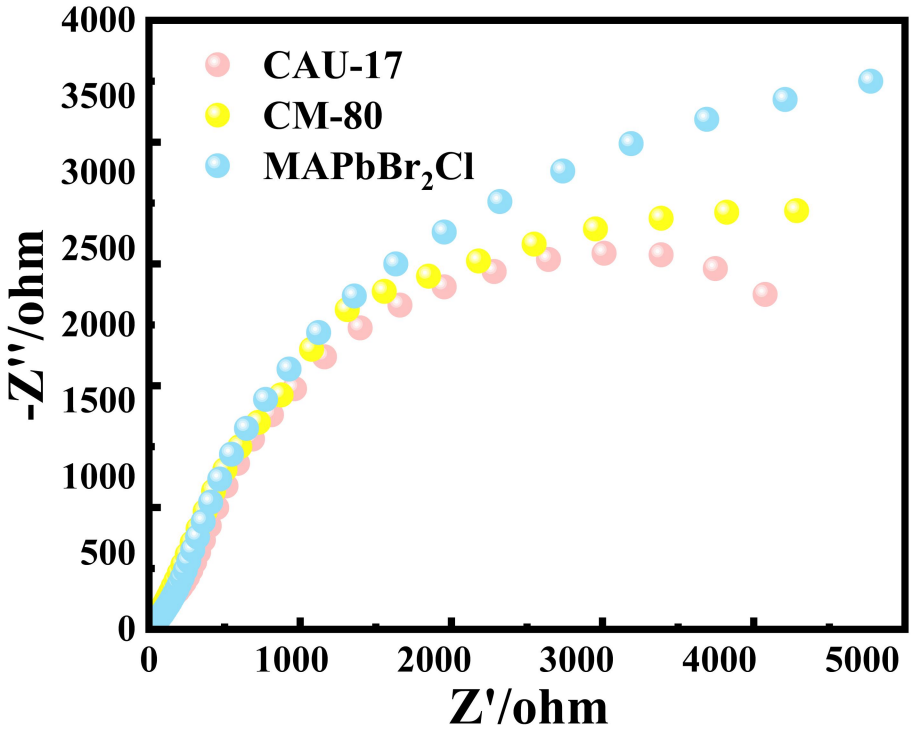

Fig.S9 EIS curves for different samples

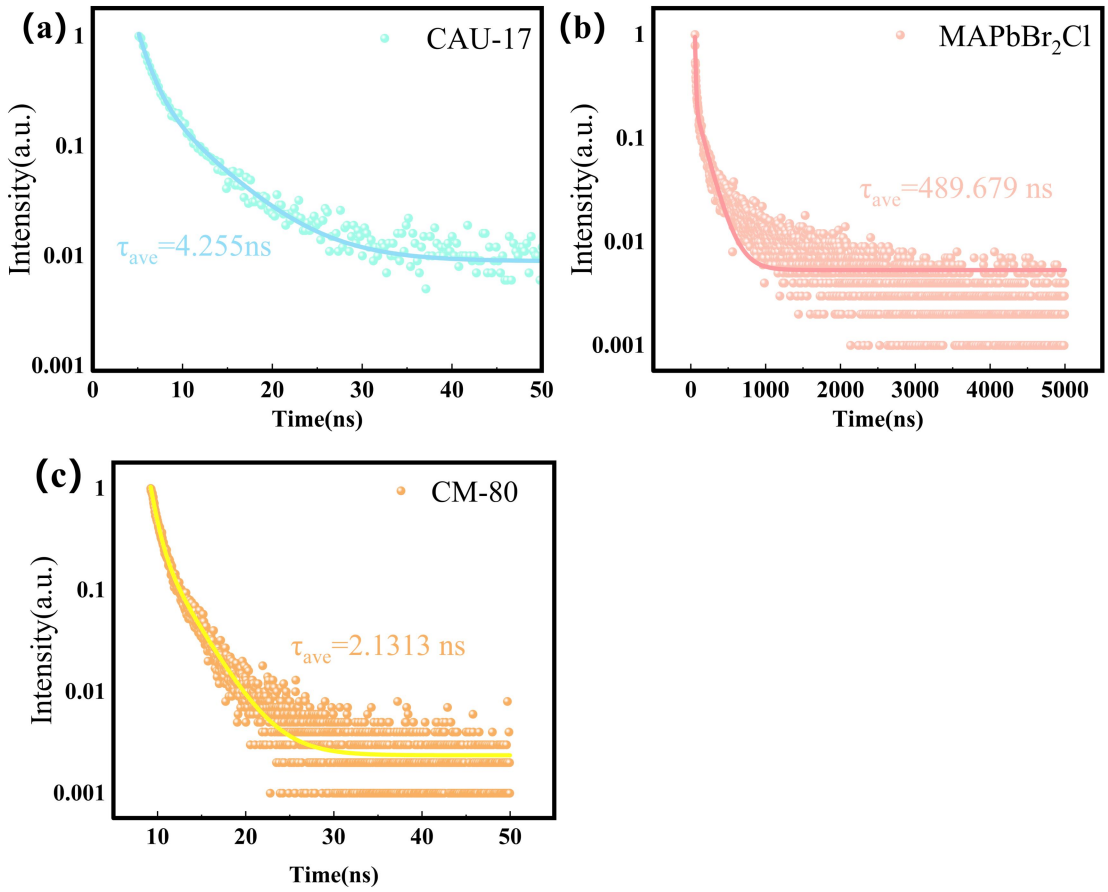

Fig.S10 Decay curves of （a）CAU-17（b）$MAPbBr_2Cl$ and （c）CM-80

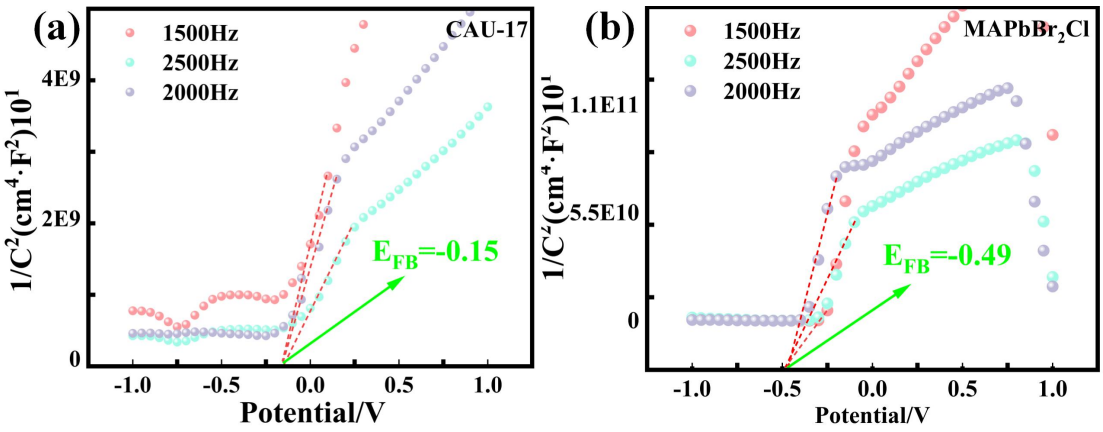

Fig.S11 Mott-Schottky diagram of (a) CAU-17 and (b) $MAPbBr_2Cl$

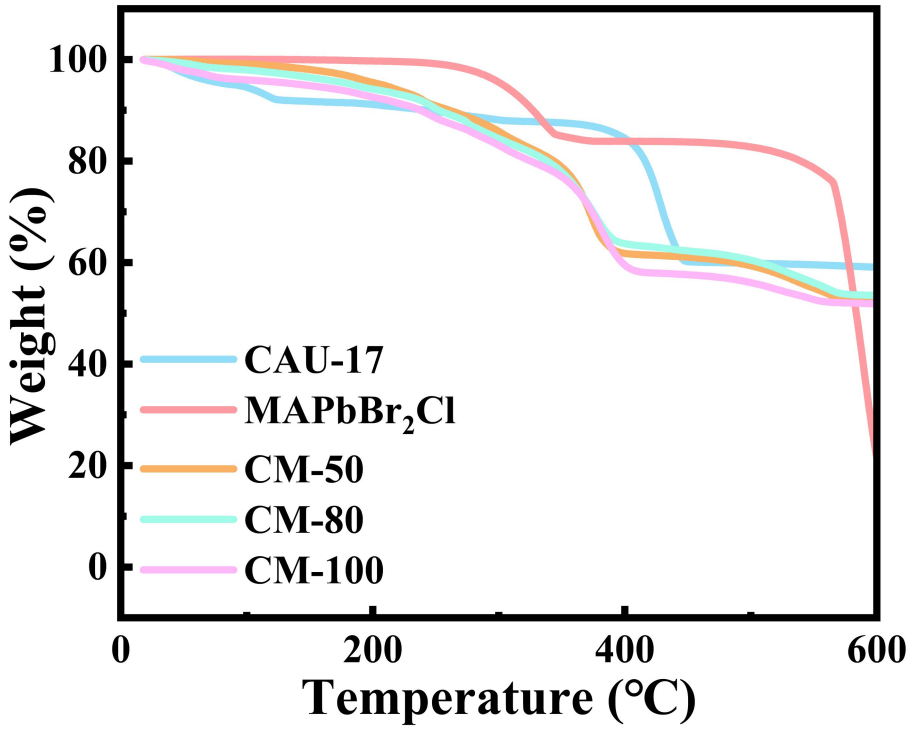

Fig.S12 TG curve of the prepared material

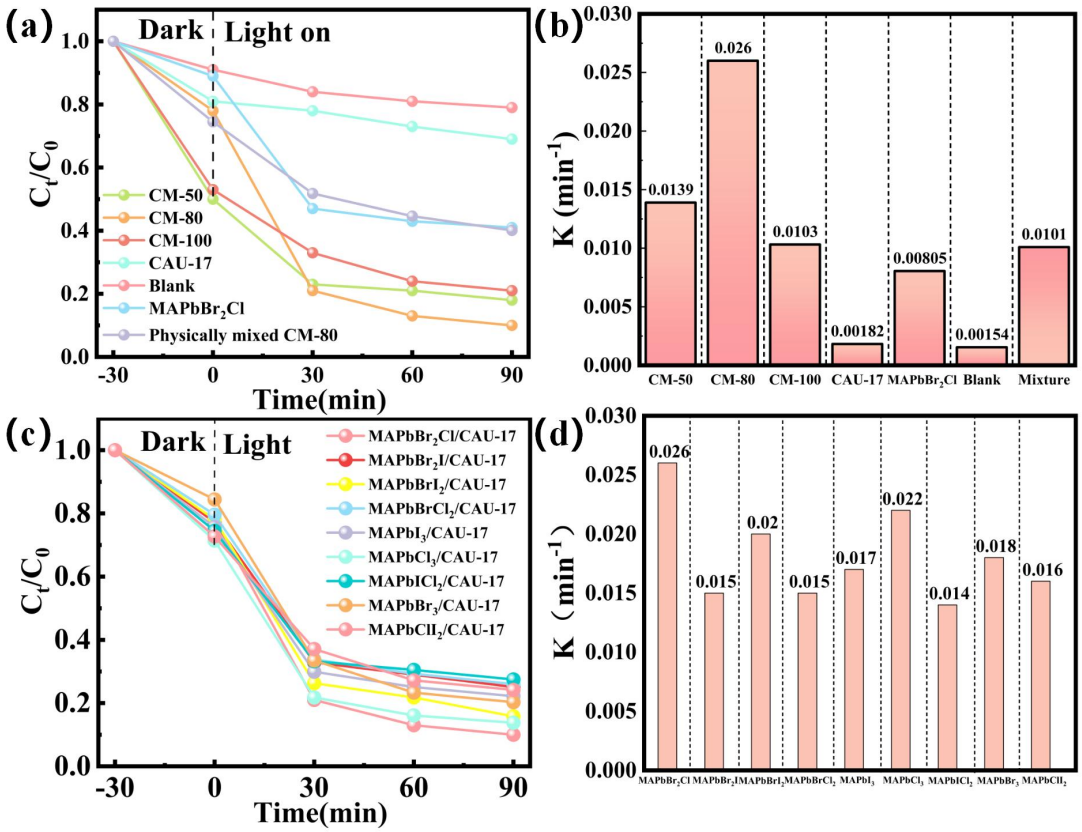

Fig.13 (a) Degradation performance of TC by different materials under visible light; (b) Kinetic rates of different photocatalysts; (c) The degradation performance of different halogen ion substituted $MAPbBr_3$ and CAU-17 complex TC; (d) Kinetic rates of $MAPbBr_3$ and CAU-17 composites with different halogen ion substitutions (experimental conditions :[TC]=80 mL, 10 mg·L^{-1}; Dosage of photocatalyst: 20 mg; Temperature = 25±0.5℃)

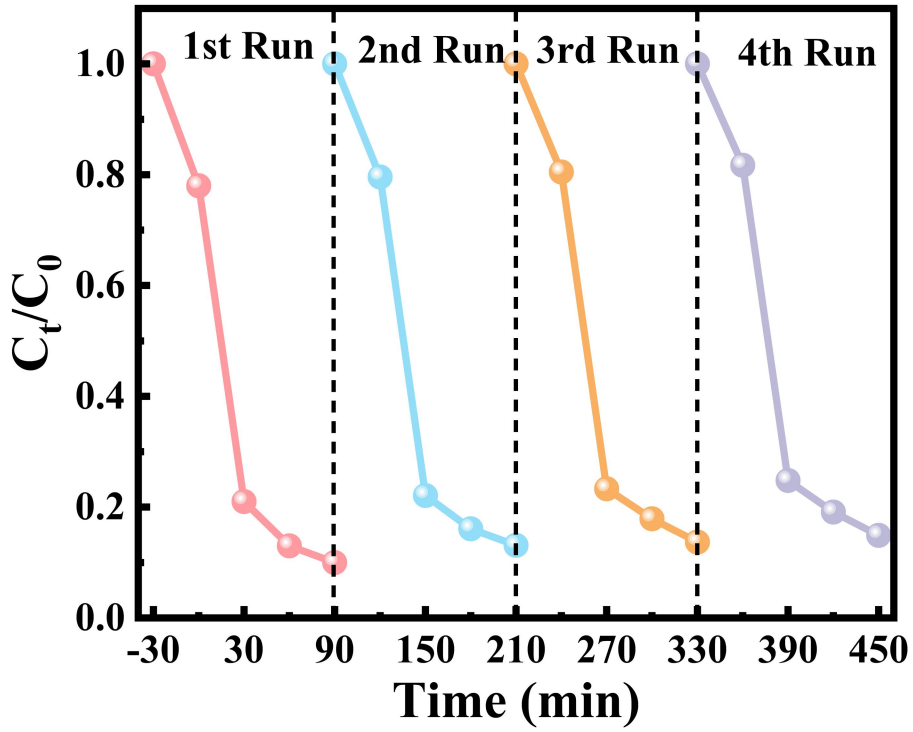

Fig.S14 CM-80 Cyclic experiment of photocatalytic degradation of TC (experimental conditions: [TC]=10 mg·L^{-1}, amount of photocatalyst =20 mg, temperature = 25±0.5℃)

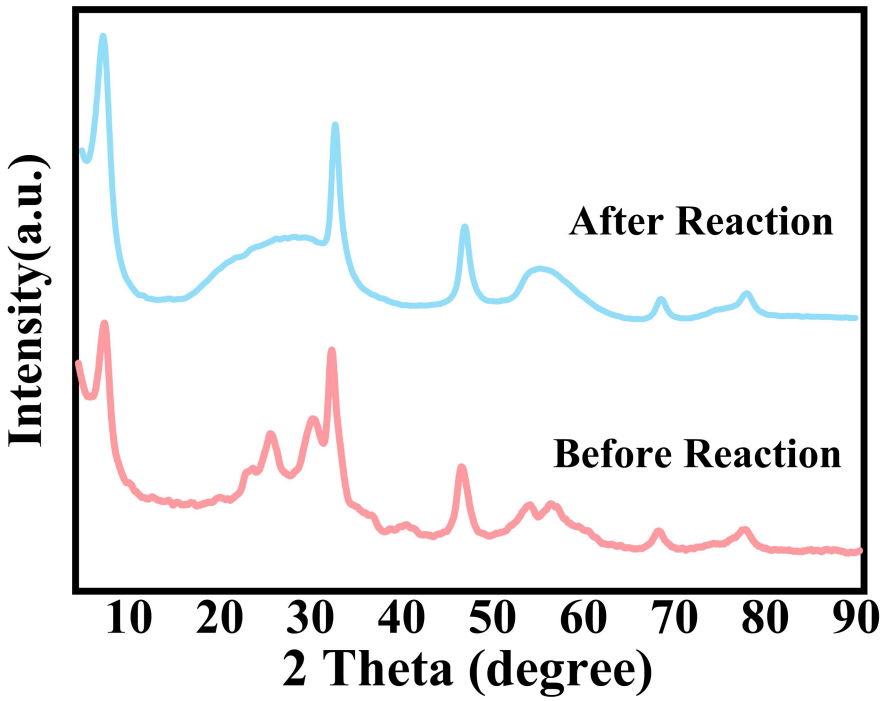

Fig.S15 XRD of CM-80 before and after the reaction

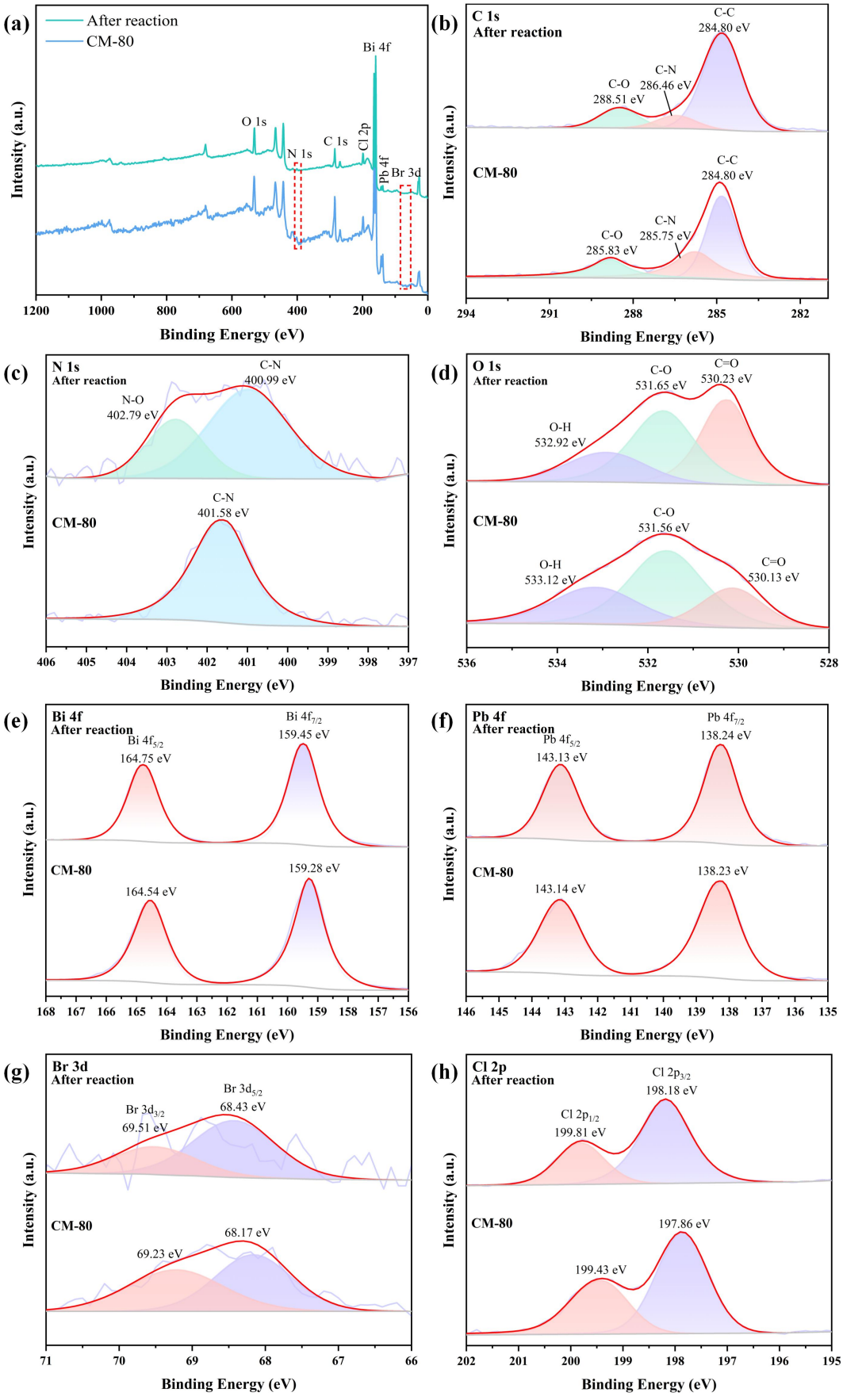

Fig.S16 XPS of CM-80 before and after the reaction

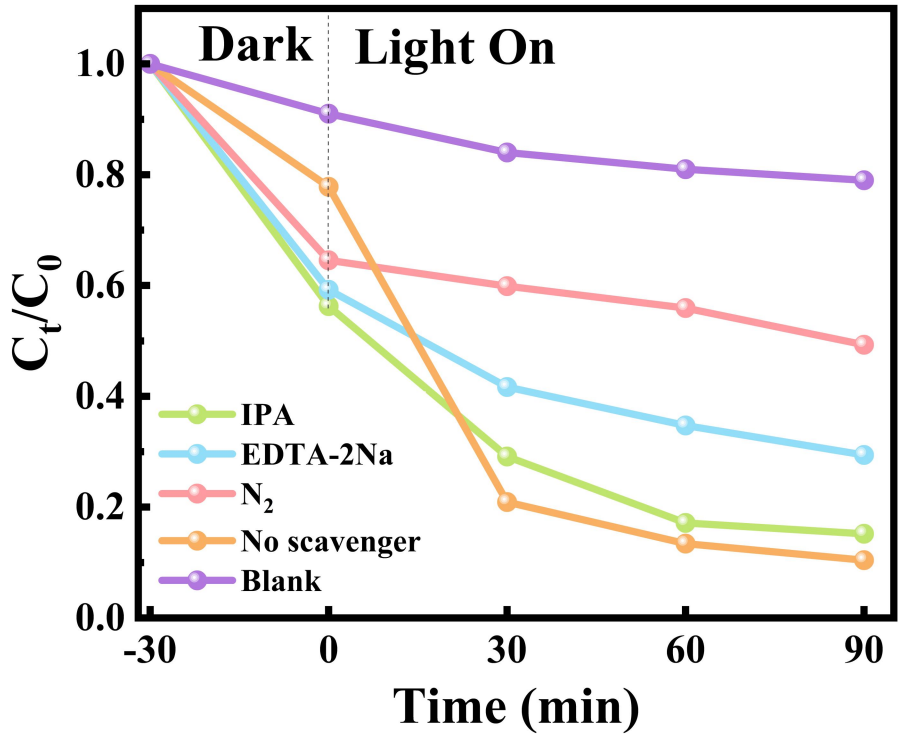

Fig.S17 Effects of different masking agents on photocatalytic degradation of TC of CM-80 composites

(Reaction condition: 1 mM of masking agent was added to 80mL of TC solution with a concentration of 80mg/L)

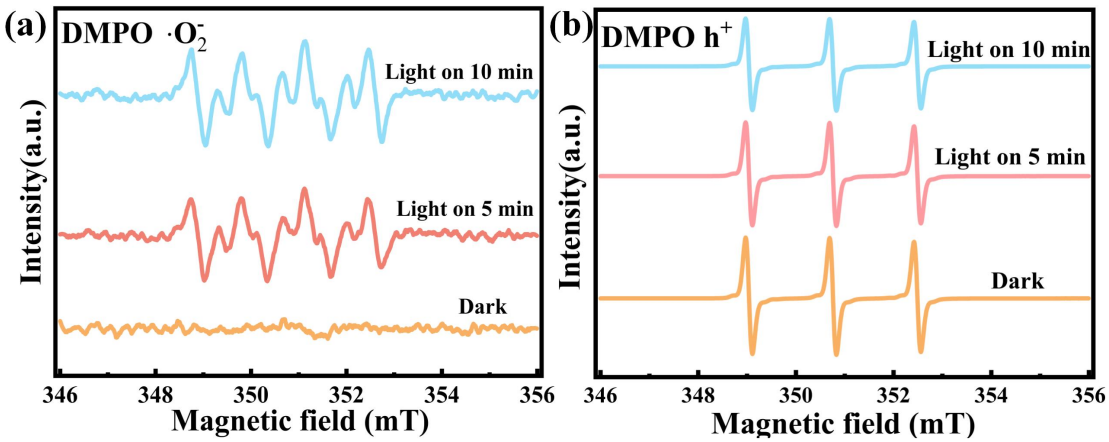

Fig.S18 ESR spectra of CM-80 composites under dark and visible light irradiation: (a) h^+, (b) $\cdot O_2^-$

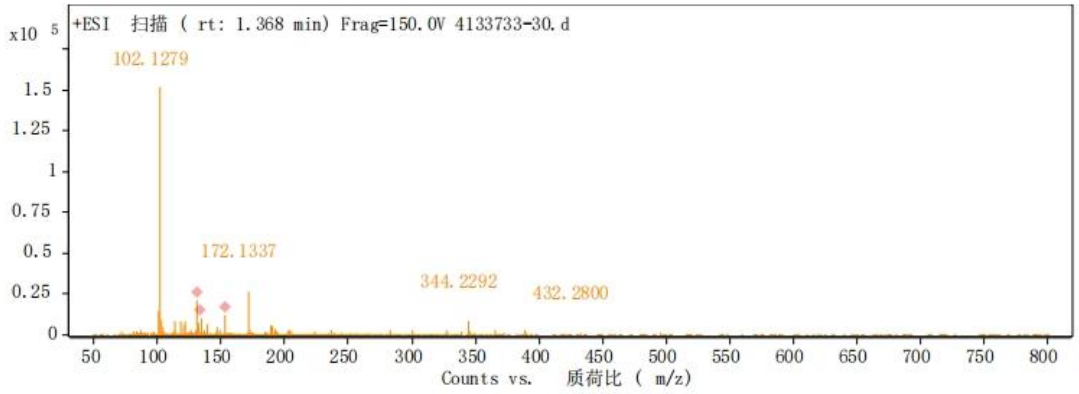
+ESI 扫描 (rt: 1.368 min) Frag=150.0V 4133733-30.d
x10 5
102.1279
172.1337
344.2292
432.2800
Counts vs. 质荷比 (m/z)

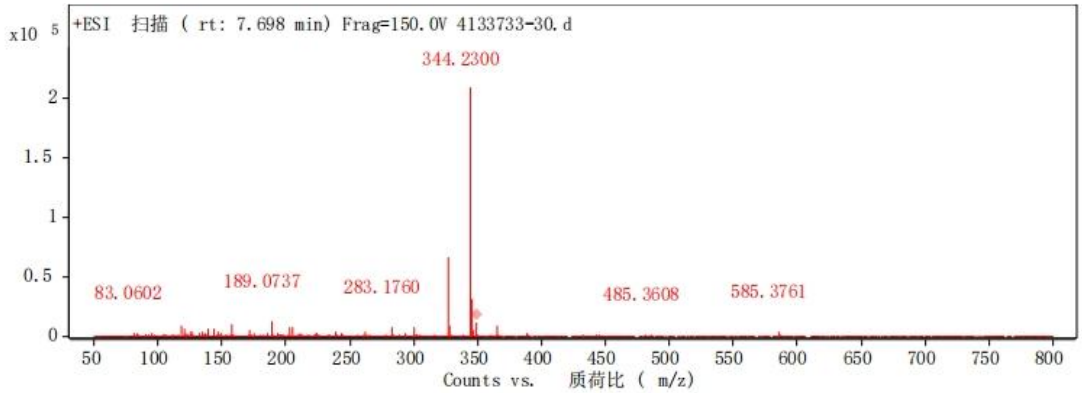
+ESI 扫描 (rt: 7.698 min) Frag=150.0V 4133733-30.d
x10 5
344.2300
83.0602
189.0737
283.1760
485.3608
585.3761
Counts vs. 质荷比 (m/z)

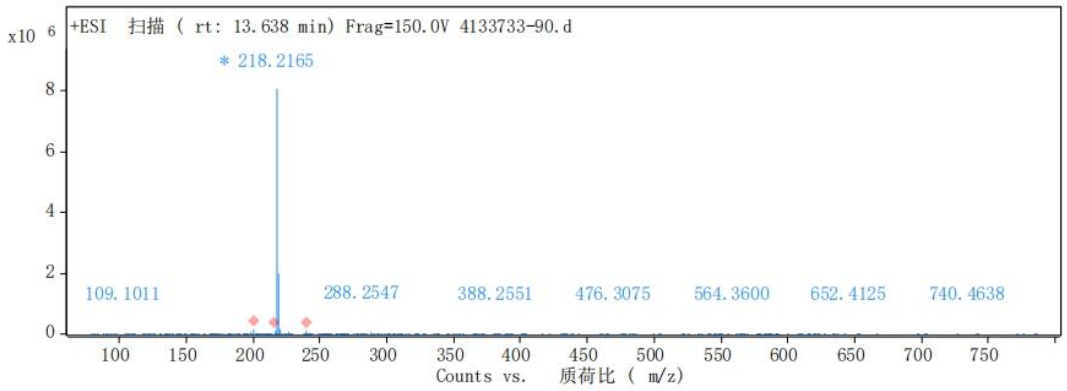
+ESI 扫描 (rt: 13.638 min) Frag=150.0V 4133733-90.d
x10 6
* 218.2165
109.1011
288.2547
388.2551
476.3075
564.3600
652.4125
740.4638
Counts vs. 质荷比 (m/z)

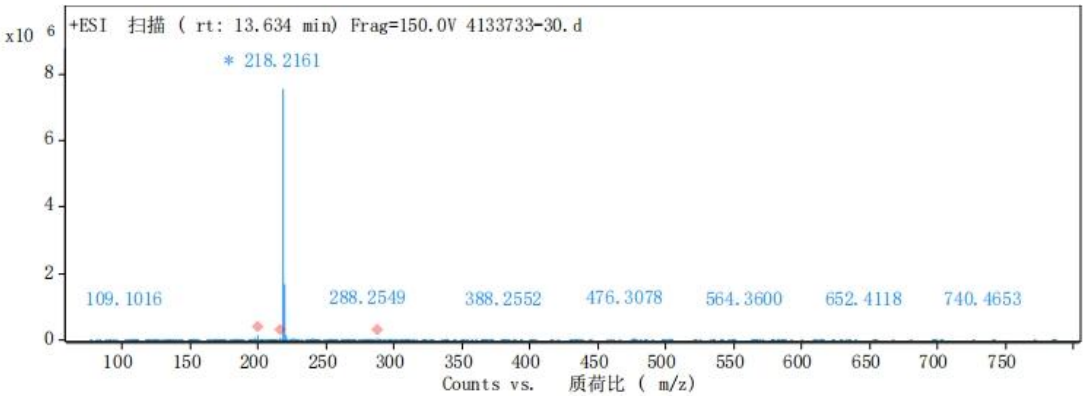
+ESI 扫描 (rt: 13.634 min) Frag=150.0V 4133733-30.d
x10 6
* 218.2161
109.1016
288.2549
388.2552
476.3078
564.3600
652.4118
740.4653
Counts vs. 质荷比 (m/z)

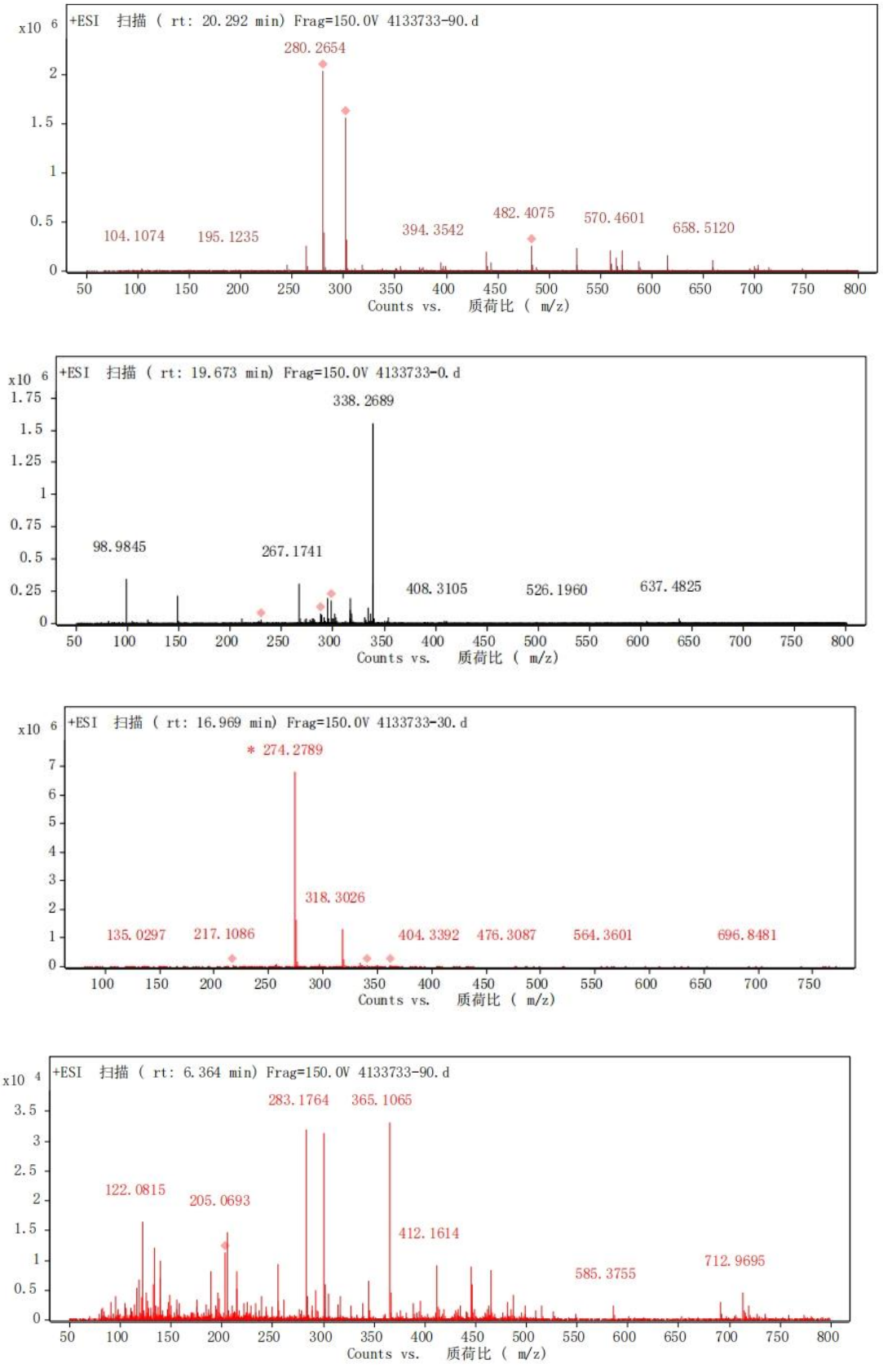

Fig.S19. LC-MS diagrams at different times

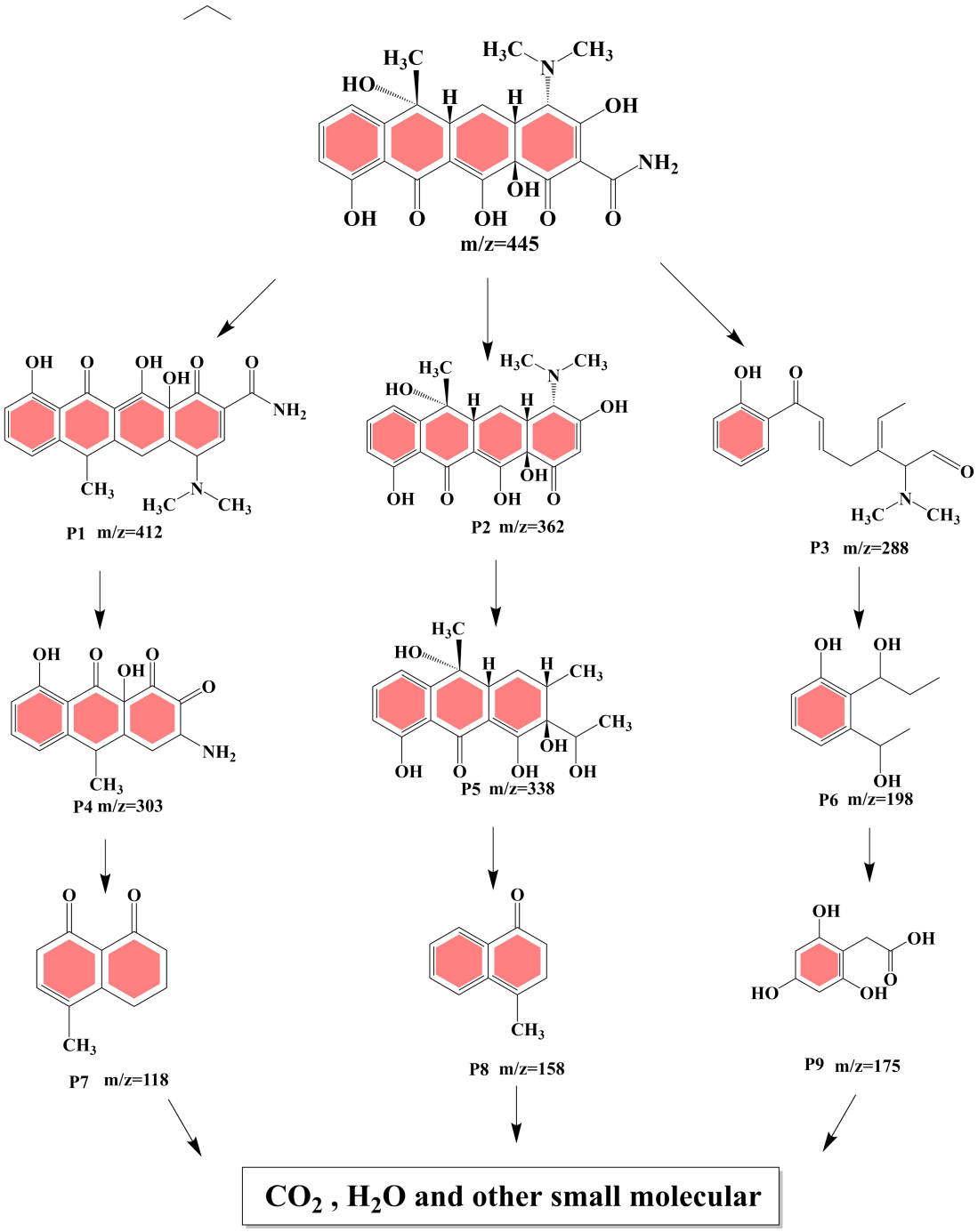

Fig.S20 Possible TC degradation paths of CM-80 composites

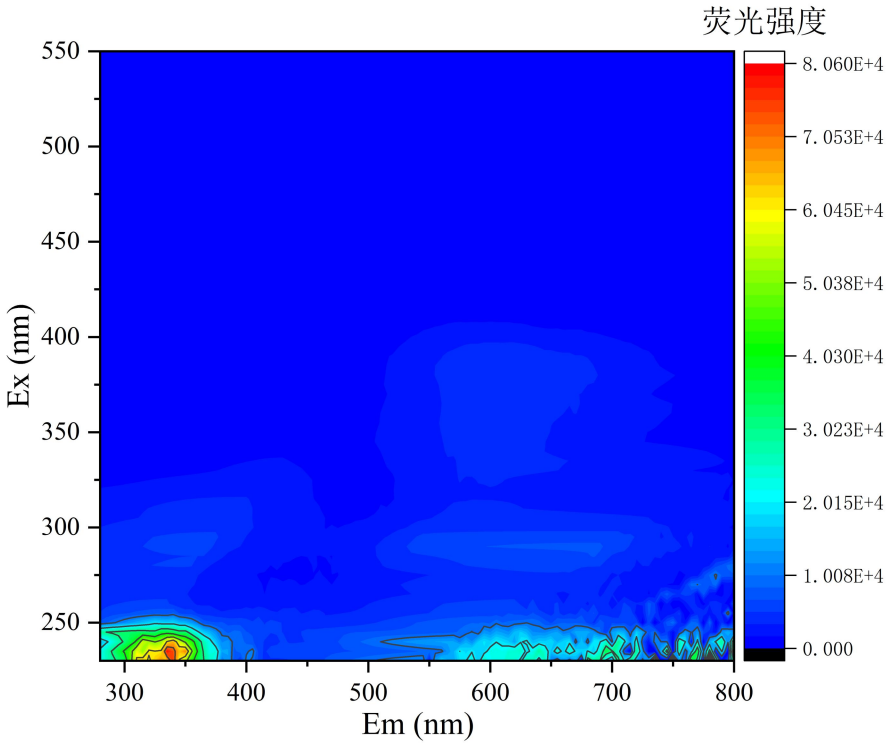

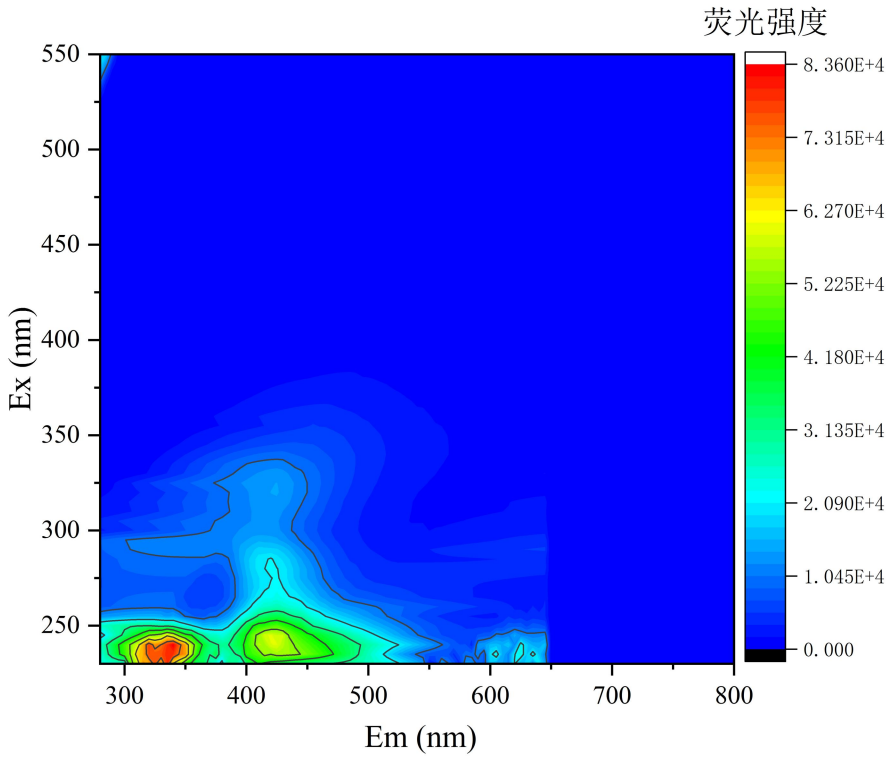

Figure S21. Three-dimensional fluorescence images of TC before and after degradation

\\

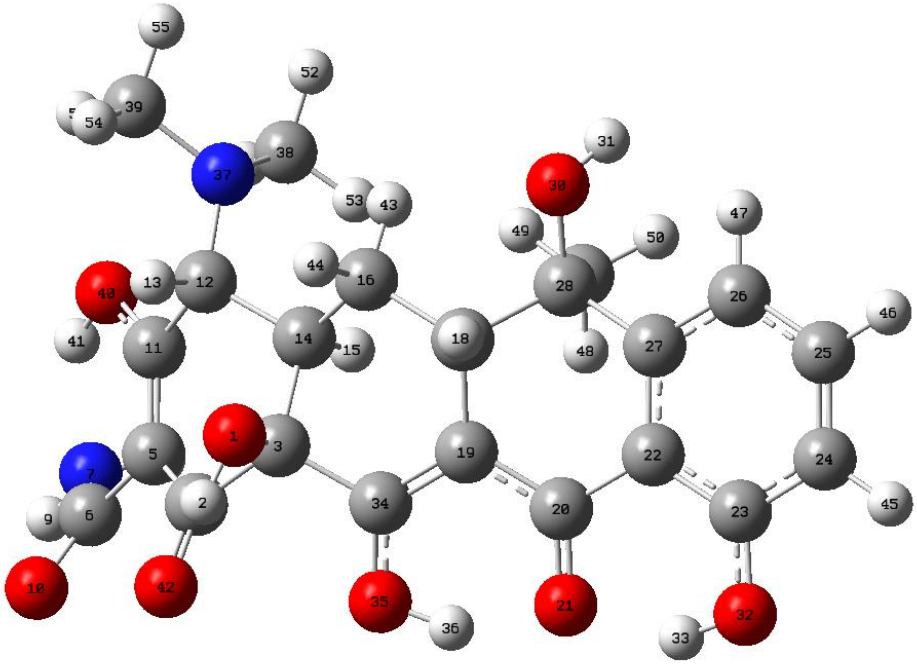

Figure S22. TC optimized organization

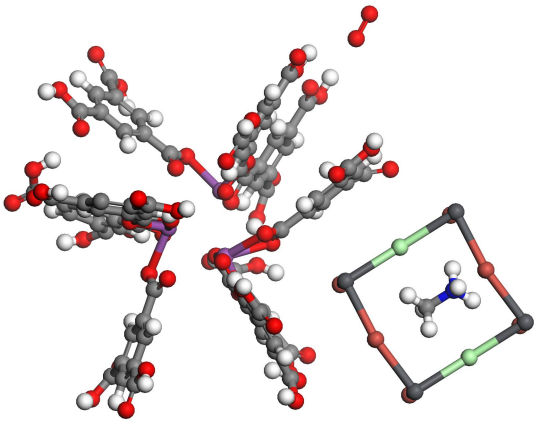

Figure S23. Model cross-section

(a)

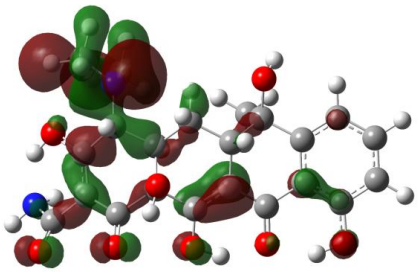

(b)

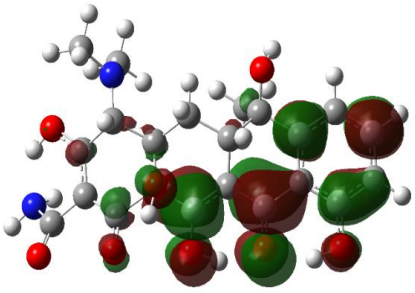

(c)

No.	Atom	q(N)	q(N+1)	q(N-1)	f⁻	f⁺
1	O	-0.21	-0.24	-0.2	0.011	0.025
2	H	0.16	0.148	0.17	0.01	0.012
3	C	0.07	0.062	0.073	0.003	0.008
4	C	0.136	0.113	0.14	0.004	0.023
5	C	-0.08	-0.09	-0.07	0.013	0.013
6	C	0.173	0.162	0.181	0.008	0.011
7	N	-0.14	-0.15	-0.13	0.01	0.011
8	H	0.129	0.123	0.134	0.005	0.006
9	H	0.133	0.118	0.145	0.013	0.015
10	O	-0.25	-0.28	-0.22	0.031	0.029
11	C	0.117	0.077	0.12	0.003	0.04
12	C	0.028	0.022	0.037	0.009	0.006
13	H	0.047	0.035	0.058	0.011	0.012
14	C	-0.03	-0.03	-0.02	0.003	0.002
15	H	0.023	0.019	0.027	0.005	0.004
16	C	-0.05	-0.06	-0.05	0.003	0.005
17	C	-0.02	-0.02	-0.01	0.005	0.003
18	H	0.037	0.026	0.05	0.013	0.01
19	C	-0.06	-0.08	-0.03	0.036	0.017
20	C	0.126	0.054	0.134	0.007	0.072
21	O	-0.23	-0.29	-0.21	0.019	0.066
22	C	-0.05	-0.05	-0.02	0.029	0.009
23	C	0.099	0.071	0.132	0.033	0.028
24	C	-0.06	-0.09	-0.03	0.035	0.031
25	C	-0.02	-0.08	0.006	0.03	0.054
26	C	-0.07	-0.09	-0.02	0.048	0.024
27	C	0.003	-0.02	0.014	0.011	0.026
28	C	0.087	0.086	0.09	0.002	0.002
29	C	-0.09	-0.1	-0.09	0.004	0.005
30	O	-0.22	-0.23	-0.21	0.009	0.012
31	H	0.16	0.149	0.169	0.009	0.011
32	O	-0.19	-0.23	-0.13	0.065	0.035
33	H	0.136	0.125	0.151	0.015	0.011
34	C	0.111	0.056	0.134	0.024	0.054
35	O	-0.16	-0.21	-0.13	0.038	0.048
36	H	0.138	0.123	0.148	0.01	0.014
37	N	-0.09	-0.09	0.008	0.098	0.001
38	C	-0.04	-0.05	-0.02	0.02	0.003
39	C	-0.04	-0.05	-0.02	0.023	0.005
40	O	-0.15	-0.18	-0.15	0.004	0.032
41	H	0.138	0.127	0.146	0.008	0.011
42	O	-0.23	-0.28	-0.2	0.029	0.041
43	H	0.025	0.015	0.03	0.004	0.011
44	H	0.035	0.025	0.043	0.009	0.01
45	H	0.05	0.028	0.072	0.022	0.023
46	H	0.049	0.021	0.071	0.021	0.028
47	H	0.036	0.017	0.056	0.02	0.018
48	H	0.033	0.032	0.036	0.003	0.001
49	H	0.031	0.021	0.034	0.004	0.009
50	H	0.031	0.019	0.042	0.01	0.012
51	H	0.014	0.007	0.047	0.033	0.007
52	H	0.035	0.024	0.056	0.021	0.011
53	H	0.03	0.032	0.043	0.013	0
54	H	0.036	0.031	0.055	0.019	0.005
55	H	0.033	0.023	0.056	0.022	0.011
56	H	0.017	0.01	0.052	0.035	0.008

Figure S24. Hirshfeld charge distribution of TC's (a) HOMO (b) LUMO's equidensity surface (c) Fukui index

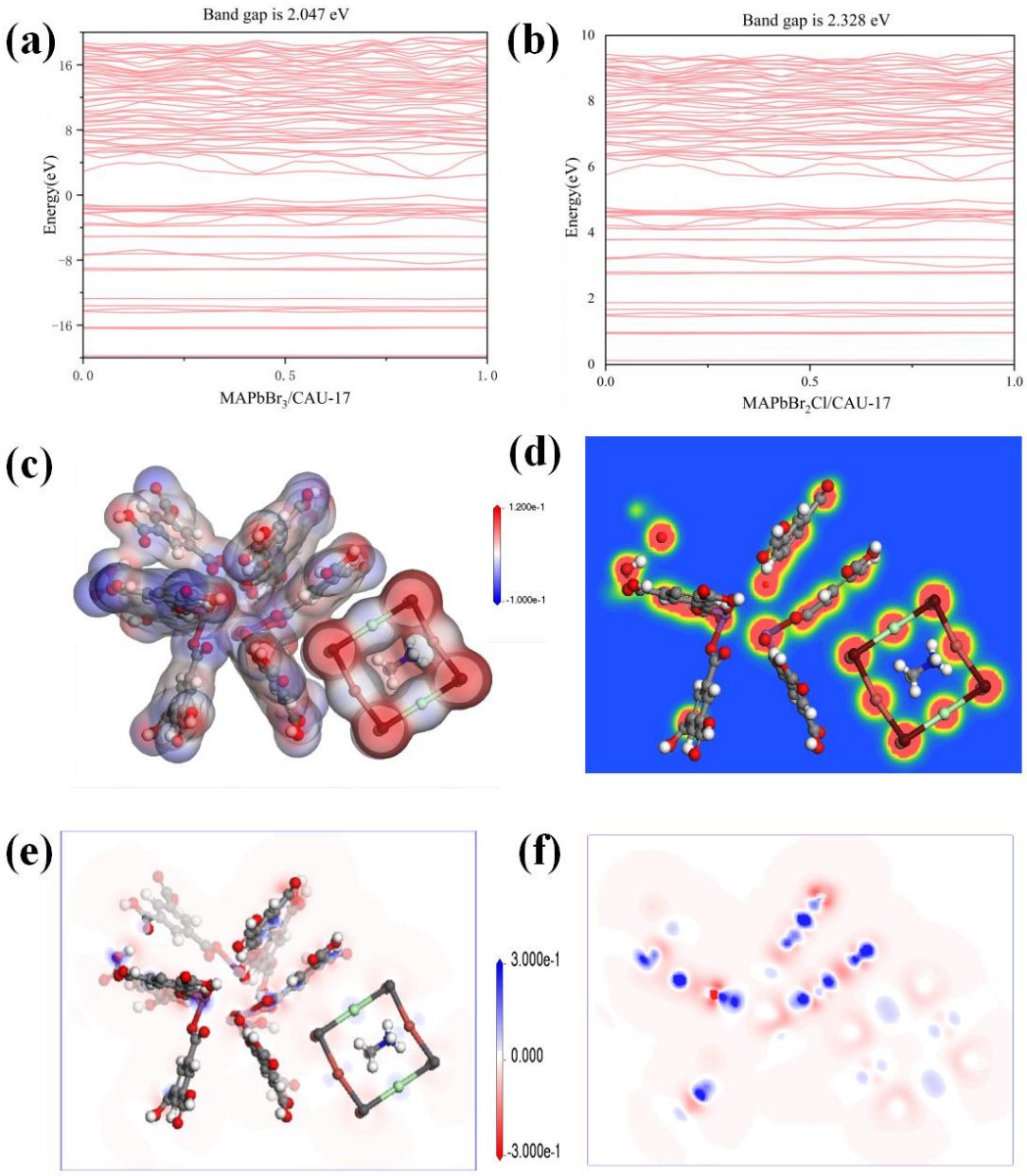

Fig. S25 Band structure of (a) $MAPbBr_3$/CAU-17 and (b) $MAPbBr_2Cl$/CAU-17 of CM-80 composites; (c-d) $MAPbBr_2Cl$/CAU-17 charge density diagram; (e-f) Differential charge density diagram (red: O, white: H, gray: C, brownish-red: Pb, light brown: Br, green: Cl)